J. Phys. Chem. A **2009,** *113,* 8529–8532

Minimum Enhancement of Surface-Enhanced Raman Scattering for Single-Molecule Detections

Geun Hoi Gu and Jung Sang Suh*

Nano-materials Laboratory, Department of Chemistry, Seoul National University, Kwanak-ro 599, Kwanak-gu, Seoul 151-747, Republic of Korea

Received: March 25, 2009; Revised Manuscript Received: June 8, 2009

We have calculated the minimum enhancement factor for single-molecule detections from the surface-enhanced Raman scattering (SERS) data measured from well-defined silver nanorod arrays. Silver nanorods were fabricated by electrodepositing them evenly near the mouth of the pores of anodic aluminum oxide templates with a very shallow depth. The SERS intensity increased almost linearly with an increase in the concentration of the mother solution. From the data of the enhancement and the number of molecules irradiated by the laser beam at the detection limit, the minimum SERS enhancement factor for nonresonant single-molecule detections was calculated to be approximately 10^{11}.

Introduction

Surface-enhanced Raman scattering (SERS) is emerging as a probing technique for biosensors because of its high sensitivity.[1−8] It is known that SERS has the sensitivity to detect even single molecules.[9−15] On the basis of early reports, a very high surface enhancement of up to $10^{14}-10^{15}$ may be required for single-molecule detections.[9,10] Since the early reports, the minimum enhancement factors for single-molecule detections have been studied theoretically and experimentally.[16−24] The newly reported minimum enhancement factors for single-molecule detections are in a wide range, $\sim10^5-10^{12}$.[16−24] This wide range of values may result from the uncertainties in the measurements of the Raman intensities and the estimation of the number of molecules adsorbed on the surface. For example, there is a big discrepancy between the enhancements calculated by a comparison of the SERS intensity to the normal Raman intensity and by a comparison of Stokes and anti-Stokes SERS intensities to those of normal Raman.[25] Most of the minimum enhancement factors were calculated from the SERS data measured from silver colloids. However, in several aspects, colloids are not proper as a SERS substrate for accurate enhancement measurements: (i) aggregation of colloids, which affects the enhancement, is very hard to control; (ii) it is almost impossible to control the adsorption sites, which also affect the enhancement, of molecules on the aggregated colloids; (iii) the collection of SERS signals from colloid solutions is not stable because of Brownian motion of the colloids or changing aggregation of the colloids.

Silver nanorods fabricated in the pores of anodic aluminum oxide (AAO) templates are very uniform in diameter and length and very reproducible.[25−29] Also, their structure does not change when molecules are adsorbed because they are fixed in the pores. Finally, molecules are adsorbed only on one end of the nanorods because they are surrounded with oxide, except for their top tips. Therefore, the silver nanorods fabricated in the pores of AAO templates may be ideal substrates for precise measurements of SERS enhancement.

In this study, we have fabricated silver nanorod arrays by electrodepositing nanorods evenly near the mouth of the pores of AAO templates with a very shallow depth and used them to study SERS by varying the concentration of the adsorbate. From the data of the enhancement measured and the concentration of the detection limit, we suggested the minimum enhancement for nonresonant single-molecule detection using SERS.

Experimental Section

A highly ordered porous AAO template was fabricated by using a two-step anodization technique. Clean aluminum sheets (99.999%, 0.5 mm thickness, Goodfellow Ltd.) were anodized in 0.3 M sulfuric acid at 10 °C and at a constant applied voltage of 25 V for 24 h after annealing and electropolishing. The resultant aluminum oxide film was subsequently removed by dipping of the anodized sheet into an aqueous mixture of chromic acid (1.8 wt %) and phosphoric acid (6 wt %) for 16 h at 60 °C. The second anodization was performed for 35 s under the same conditions as those of the first. The pore diameter was widened by etching in a 0.1 M phosphoric acid solution at 30 °C for 15 min. The thickness of the oxide film including the bottom barrier was approximately 95 nm. Silver nanorods were deposited in the pores of the films by applying an alternating-current voltage of 14 V with a frequency of 200 Hz for 20 s in an ethanol solution containing 0.05 M $AgNO_3$ (99.9999%, Aldrich) at 5 °C (see Figure 1). The AAO film, upon which the silver nanorods were deposited on both sides, was cut into several (1 cm × 0.5 cm) pieces. Each piece was dipped into a (9.0 mL) diluted solution of *p*-aminothiophenol for 24 h and then dried for Raman measurements after the surface was washed with ethanol. Raman spectra were observed by using a micro-Raman system equipped with a homemade sample stage, a monochromator (SPEX 500 M), and a CCD camera cooled with liquid nitrogen (Roger Scientific model 7346-001). SERS and normal Raman spectra were observed by excitation with a 514.5-nm laser line. The incident laser power on the sample was approximately 100 μW, and the acquisition time was 10 or 100 s. The Raman spectrum of liquid *p*-aminothiophenol (the material's melting point: 37 °C) was observed by containing it in a capillary (100 μm in diameter). The Raman frequencies were corrected by using the Raman peaks of a mixture of toluene

---

* Author to whom correspondence should be addressed. E-mail: jssuh@snu.ac.kr.

10.1021/jp902714t CCC: $40.75

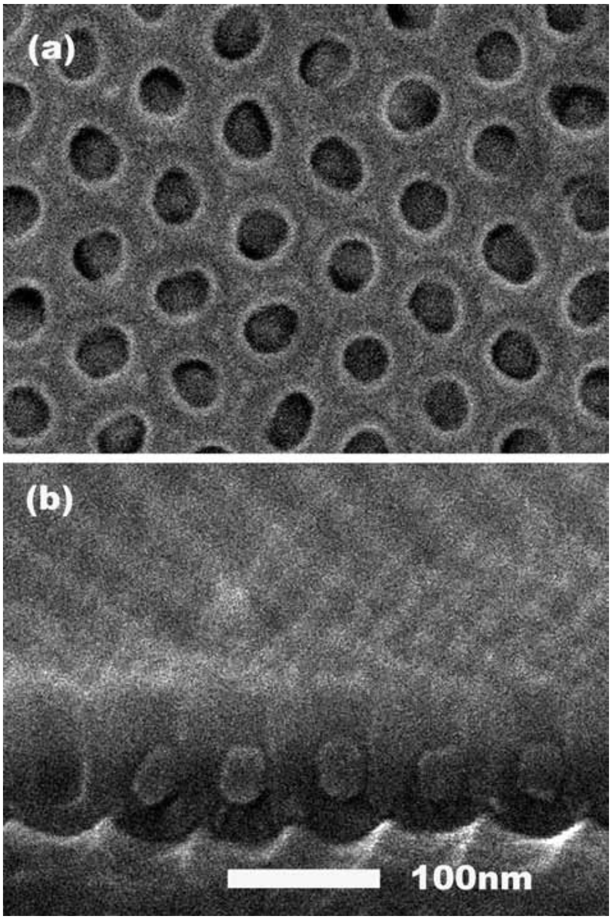

Figure 1. SEM images of the silver nanorods electrodeposited in the pore of an AAO template: (a) top view; (b) side view.

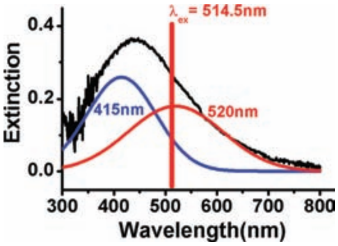

Figure 2. Extinction spectrum (black line) of silver nanorod arrays and deconvoluted spectra (blue and red lines). The diameter and length of the silver nanorods were 28 and 44 nm, respectively.

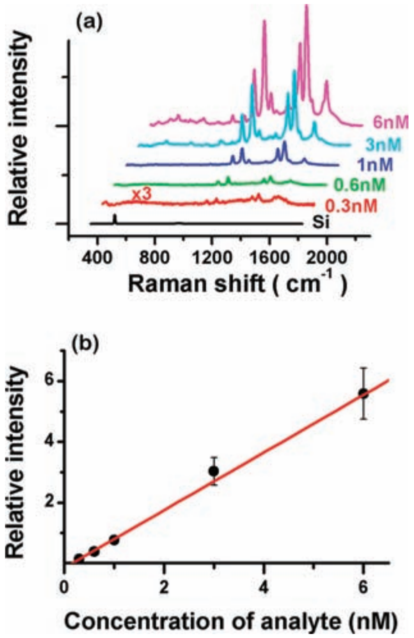

Figure 3. (a) SERS spectra of *p*-aminothiophenol adsorbed onto the tips of the silver nanorods observed by excitation with a 514.5-nm laser line. (b) Intensity profile of the peak at 1077 cm^{-1} as a function of the concentration of the adsorbate mother solutions. The straight line was obtained by a linear fitting, and the error bars are shown. The values labeled on the right-hand side in part a are the concentrations of the mother solutions.

and acetonitrile (1:1, v/v). The UV−visible extinction spectrum of the silver nanorod arrays fabricated on an AAO template was measured by a reflection method using a Cary Varian 300 Bio/diffuse-reflectance kit. The spectrum was deconvoluted by a Gaussian fitting using the *Origin* program (6.1 version). The fabricated templates and nanorods were analyzed by scanning electron microscopy [SEM; JEOL ltd. JSM6700F (10 kV)].

p-Aminothiophenol, toluene, and acetonitrile were obtained from Sigma-Aldrich and were used as received. All of the glassware was cleaned by dipping in a cleaning solution, washing with distilled water, and then drying in an oven. Before using glassware such as a mass flask and vials, all were cleaned again by a sonicator, using a pure methanol solvent.

Results and Discussion

The SEM images of the silver nanorods deposited in the pores of the AAO template prepared in sulfuric acid are shown in Figure 1. Silver nanorods are deposited in all of the pores. They exhibit a two-dimensional array with a hexagonal pattern. The distance between the centers of the nanorods is very uniform at 65 nm. The nanorod density is approximately 2.7 × 10^{10} nanorods/cm^2. The diameter of the nanorods is uniform at approximately 28 nm. In the side view, some nanorods are not visible and some are tilted. To observe the side view of the nanorods, the AAO template was bent. The missing nanorods might have slipped out from the pores during this process because silver particles are seen in all of the pores in the top view. Also, some nanorods on the edge might have been tilted during the same process. However, the alignment of the nanorods in the pores is perfectly vertical with respect to the surface of the template. It should be mentioned that the shape of the pores looks like a funnel, consisting of a hexagonal mouth and stem. The inside shape of the mouth is closer to a half-sphere than a cone. The average length of the silver nanorods is approximately 44 nm. The full depth of the pores of the AAO template, including the mouth and stem parts, is approximately 70 nm, with the stem part itself being approximately 50 nm long.

The UV−visible extinction spectrum of the silver nanorod array fabricated on an AAO template, measured by a reflection method, is shown in Figure 2. The spectrum has been deconvoluted by a Gaussian fitting. There are two bands at 415 and 520 nm. The former is due to the transverse mode of the surface plasmon, and the latter is due to the longitudinal mode.[30] The maximum position of the longitudinal mode is very close to the 514.5-nm laser line of an argon ion laser.

The SERS spectra of *p*-aminothiophenol adsorbed onto the tips of the silver nanorods are shown in Figure 3. They were measured by excitation with a 514.5-nm laser line. Each SERS sample was prepared by dipping of a piece of the AAO template with deposited silver nanorods (1.0 cm × 0.5 cm) into 9.0 mL of an ethanol analyte solution for 24 h. Because the silver

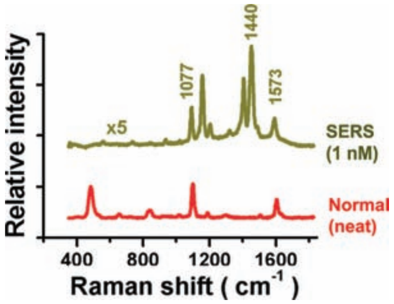

Figure 4. Comparison of the normal Raman spectrum of *p*-aminothiophenol with its SERS spectrum. Both spectra were observed by excitation with a 514.5-nm laser under the same conditions. The SERS spectrum is magnified 5 times to normalize the intensity of the peak at 1077 cm^{-1}.

nanorods are deposited on both sides of the AAO template, the total film surface area of each piece is 1 cm^2. The concentrations of the analyte solutions varied from 1.0 × 10^{-8} to 1.0 × 10^{-11} M. The SERS peaks correspond to the modes of a benzene ring.[31] For example, the peak at 1573 cm^{-1} is due to ν_{8b}, and the one at 1440 cm^{-1} is due to ν_{19b}. Moreover, the peak at 1077 cm^{-1} is due to ν_{7a} with contributions from the C−S stretching vibration (ν_{CS}). For comparison, the Raman spectrum of silicon is shown at the bottom. The intensity profile of the peak at 1077 cm^{-1} as a function of the concentration of the *p*-aminothiophenol mother solution is shown in Figure 3b. The intensity increases almost linearly to 6.0 × 10^{-9} M *p*-aminothiophenol molecules in the mother solution. It should be mentioned that the SERS intensity fluctuation, from spot to spot on a sample plate, was approximately ±7% from the average value. This value is relatively small, probably because of the uniformity of the silver nanorods and the surface concentration of the adsorbate. The silver nanorods are very uniform in diameter and length, and they exhibit a two-dimensional array with a hexagonal pattern. The molecules are adsorbed to the surface by random collision from a relatively bulk solution, and the surface concentration may become very uniform on the entire surface. In Figure 3b, the fitting straight line does not pass through the origin. The cause of the nonzero intercept is not clear. One probable cause is that, at a very low concentration of analyte, most of them could remain in the solution phase or be adsorbed onto the alumina. In this case, they will not contribute to the SERS intensity and the nonzero intercept could be observed. However, this kind of effect does not affect the value of the minimum enhancement factor for single-molecule detections. The reason will be discussed late.

We calculated the enhancement factor by comparing the intensity of the 1077 cm^{-1} peak in the SERS spectrum with that in the normal Raman spectrum by using a technique similar to that reported previously.[29] The normal Raman and SERS spectra of *p*-aminothiophenol that were observed by excitation with a 514.5-nm laser under the same conditions are shown in Figure 4. The signals were collected for 100 s by using a low-magnification objective lens (10×). The beam diameter was approximately 5 μm. It should be mentioned that, in the measurement of the enhancement factor, we used the 10× lens to observe the SERS and normal Raman spectra because, with a high-magnification lens, the laser beam does not assume a cylindrical form in the liquid sample. In such a case, it is difficult to estimate the number of molecules irradiated by the laser beam. The intensity of the normal Raman peak is very similar to that of the SERS peak magnified 5 times. The SERS sample was prepared by dipping into 9.0 mL of a 1.0 × 10^{-9} M solution.

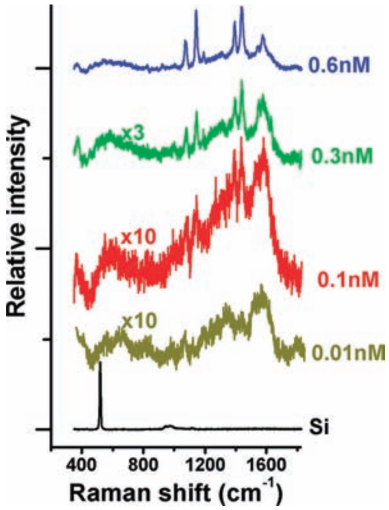

Figure 5. SERS spectra of *p*-aminothiophenol adsorbed onto the tips of the silver nanorods observed by excitation with a 514.5-nm laser line. The concentrations labeled on the right-hand side are those of mother solutions of *p*-aminothiophenol.

The number of molecules contained in this amount of the solution is 5.4 × 10^{12} molecules (6.02 × 10^{23} molecules/mol × 9.0 × 10^{-3} L × 1.0 × 10^{-9} mol/L = 5.4 × 10^{12} molecules). Under our experimental conditions, we were unable to find the exact surface concentration of the molecules. However, we have assumed that all of the molecules contained in the mother solution are adsorbed onto the tip surfaces of the silver nanorods, existing at an AAO surface of 1 cm^2. Our assumption is based on the following three facts: (i) *p*-aminothiophenol is strongly chemiadsorbed on silver; (ii) adsorption takes place for a long time (for 24 h); (iii) the amount of molecules is much less than that for a monolayer adsorption. [By a simple calculation based on the size of *p*-aminothiophenol (0.22 nm^2),[32] the percentage of the tip surface area occupied by all of the molecules is approximately 3.5%, when the sample plate was dipped in 9.0 mL of a 1.0 × 10^{-9} M solution.] The surface area irradiated by a 5-μm-diameter laser beam is 19.6 μm^2 [3.14 × (2.5 μm)^2 = 19.6 μm^2]. Therefore, 1.06 × 10^6 molecules exist in the laser beam spot [5.4 × 10^{12} molecules × 19.6 μm^2/(1 cm^2) = 1.06 × 10^6 molecules]. The normal Raman spectrum was observed for a 100-μm-thick cell filled with a pure *p*-aminothiophenol liquid that had a density of 1.06 g/cm. The molecular mass of *p*-aminothiophenol is 125.19 g/mol. The probe volume was approximately 1.96 × 10^3 μm^3, calculated by assuming that it is a cylinder with a diameter of 5.0 μm and a height of 100 μm [3.14 × (2.5 μm)^2 × 100 μm = 1.96 × 10^3 μm^3]. Under these conditions, 9.99 × 10^{12} molecules would be irradiated [(volume × density × Avogadro's number)/molar mass = 1.96 × 10^2 μm^3 × 1.06 g/cm^3 × (6.02 × 10^{23} molecules/mol)/(125.19 g/mol) = 9.99 × 10^{12} molecules]. From these data of the relative intensity and the number of molecules sampled from the normal Raman and SERS measurements, the enhancement factor is calculated to be approximately 1.9 × 10^6 {(number of molecules irradiated in measuring the normal Raman spectrum/that for SERS spectrum) × intensity ratio = [(9.99 × 10^{12} molecules)/(1.06 × 10^6 molecules)] × $^1/_5$ = 1.9 × 10^6}. We believe that enhancement of 1.9 × 10^6 is due to the electromagnetic effect because it is known that the peak of *p*-aminothiophenol at 1077 cm^{-1}, which has been monitored, does not show any chemical effect.[31]

Figure 5 shows the SERS spectra of relatively low concentrations of *p*-aminothiophenol, adsorbed onto the tips of the silver nanorods, observed by using a 50× lens (2 μm in beam diameter) and excitation with a 514.5-nm laser line. The concentrations labeled on the right-hand side are those of the mother solutions of *p*-aminothiophenol. For the SERS spectrum of 3×10^{-10} M *p*-aminothiophenol molecules in the mother solution, the typical peaks of *p*-aminothiophenol molecules are clearly distinguishable from the background. Therefore, this concentration may be close to the limit of detection of *p*-aminothiophenol by SERS. Previously, we calculated that 1.06×10^6 molecules exist in the laser beam spot (5 μm in diameter) for the 1×10^{-9} M sample. Therefore, for the SERS spectrum of 3×10^{-10} M, 5.1×10^4 molecules would exist in the laser beam spot (2 μm in diameter); $\{1.06 \times 10^6$ molecules $\times [(3 \times 10^{-10}\text{ M})/(1 \times 10^{-9}\text{ M})] \times [(1\ \mu\text{m})^2/(2.5\ \mu\text{m})^2] = 5.1 \times 10^4$ molecules$\}$. The enhancement factor calculated previously was 1.9×10^6. Because the SERS intensity changes almost linearly at a low concentration, the same enhancement factor is expected. For the SERS spectrum of the concentration of the detection limit, the SERS signals are collected from 5.1×10^4 molecules at an enhancement of 1.9×10^6. Therefore, by a simple calculation, a single molecule can be detected by SERS when the enhancement is approximately 10^{11} ($5.1 \times 10^4 \times 1.9 \times 10^6 = 9.7 \times 10^{10}$). Because *p*-aminothiophenol has no absorption in the visible and is a nonresonant molecule, this value may correspond approximately to the minimum enhancement for nonresonant single-molecule detection using SERS. The minimum enhancement factor for resonant molecules would be $\sim 10^8$ if we consider the resonance factor of molecules as 10^3. This value aligned roughly with the value reported.[18]

Our silver nanorods are very uniform in size and well-ordered, and their structure does not change when molecules are adsorbed because they are fixed in the pores. Also, no treatment like etching away the oxide is needed after adsorption of molecules onto the tips of the silver nanorods. Therefore, our measurement is well-controlled and reliable. However, there is one uncertain thing: we do not know the exact surface concentration of the molecules because some molecules could remain in the solution phase or be adsorbed on alumina. In previous calculations, we have assumed that all of the molecules contained in the mother solution are adsorbed onto the tips of the silver nanorods. However, this assumption does not affect the value of the minimum enhancement factor for single-molecule detections. The SERS intensity increases almost linearly to 6.0×10^{-9} M *p*-aminothiophenol molecules in the mother solution. This means that the concentration ratio of the molecules adsorbed on the silver nanorods to those existing in the solution or adsorbed on the alumina is constant up to this concentration. The value of the minimum enhancement factor for single-molecule detections is obtained from the product of the enhancement value by the number of molecules irradiated under the detection limit. However, the enhancement value is calculated by dividing some value with the number of molecules adsorbed onto the silver nanorods irradiated by the laser beam. Therefore, in the end, the concentration ratios cancel out in the calculation of the minimum enhancement factor for single-molecule detections.

Conclusions

We have developed a technique to deposit silver nanorods evenly near the mouth of the pores of AAO templates whose depth is very shallow. Using this technique, we have fabricated silver nanorod arrays of 44 nm length, whose longitudinal mode has its maximum near 520 nm. A good SERS spectrum was observed by excitation with a 514.5-nm laser line. The SERS intensity of *p*-aminothiophenol adsorbed onto the tips of the silver nanorods changed almost linearly with the concentration of the mother solution of *p*-aminothiophenol. For the SERS spectrum of the concentration of the detection limit, the SERS signals were collected from 5.1×10^4 molecules at an enhancement of 1.9×10^6. On the basis of the enhancement and number of molecules at the limit of detection, it is suggested that the minimum SERS enhancement factor for nonresonant single molecules is approximately 10^{11}. For resonant molecules, it would be approximately 10^8.

Acknowledgment. The authors are grateful for financial support of KOSEF through CNNC and of the BK21 program.

References and Notes

(1) Cao, Y. C.; Jin, R.; Mirkin, C. A. *Science* **2002**, *297*, 1536.

(2) Shafer-Peltier, K. E.; Haynes, C. L.; Glucksberg, M. R.; Van Duyne, R. P. *J. Am. Chem. Soc.* **2003**, *125*, 588.

(3) Grubisha, D. S.; Lipert, R. J.; Park, H. Y.; Driskell, J. D.; Porter, M. *Anal. Chem.* **2003**, *75*, 5936.

(4) Nam, J. M.; Stoeva, S. I.; Mirkin, C. A. *J. Am. Chem. Soc.* **2004**, *126*, 5932.

(5) Lyandres, O.; Shah, N. C.; Yonzon, C. R.; Walsh, J. T., Jr.; Gluckberg, M. R.; Van Duyne, R. P. *Anal. Chem.* **2005**, *77*, 6134.

(6) Kneipp, J.; Kneipp, H.; Rice, W. L.; Kneipp, K. *Anal. Chem.* **2005**, *77*, 2381.

(7) Grudisha, D. S.; Lipert, R. J.; Park, H. Y.; Driskell, J.; Porter, M. D. *Anal. Chem.* **2003**, *75*, 5936.

(8) Premasiri, W. R.; Moir, D. T.; Klempner, M. S.; Krieger, N.; Jones, G.; Ziegler, L. D. *J. Phys. Chem. B* **2005**, *109*, 312.

(9) Nie, S.; Emory, S. R. *Science* **1997**, *275*, 1102.

(10) Kneipp, K.; Wang, Y.; Kneipp, H.; Perlman, L. T.; Itzkan, I.; Dasari, R. R.; Feld, M. S. *Phys. Rev. Lett.* **1997**, *78*, 1667.

(11) Kneipp, K.; Kneipp, H.; deinum, G.; Itzkan, I.; Dasari, R. R.; Feld, M. S. *Appl. Spectrosc.* **1998**, *52*, 175.

(12) Kneipp, K.; Kneipp, H.; Kartha, V. B.; Manoharan, R.; Deinum, G.; Itzhan, I.; Dasari, R. R.; Feld, M. S. *Phys. Rev. E* **1998**, *57*, R6281.

(13) Svedberg, F.; Li, Z.; Xu, H.; Klall, H. *Nano Lett.* **2006**, *6*, 2639.

(14) Habuchi, S.; Cotlet, M.; Gronheid, R.; Drix, G.; Michiels, J.; Vanderleyden, J.; De Schryver, F. C.; Hofkens, J. *J. Am. Chem. Soc.* **2003**, *125*, 8446.

(15) Le Ru, E. C.; Meyer, M.; Etchegoin, P. G. *J. Phys. Chem. B* **2006**, *110*, 1944.

(16) Kerker, M.; Wang, D. S.; Chew, H. *Appl. Opt.* **1980**, *19*, 4159.

(17) Bjerneld, E. J.; Svedberg, F.; Johansson, P.; Kall, M. *J. Phys. Chem. A* **2004**, *108*, 4187.

(18) Le Ru, E. C.; Etchegoin, P. G.; Meyer, M. *J. Chem. Phys.* **2006**, *125*, 13.

(19) Johansson, P.; Xu, H. X.; Kall, M. *Phys. Rev. B* **2005**, *72*, 17.

(20) Markel, V. A.; Shalaev, V. M.; Zhang, P.; Huynh, W.; Tay, L.; Haslett, T. L.; Moskovits, M. *Phys. Rev. B* **1999**, *59*, 10903.

(21) Fang, Y.; Seong, N. H.; Dlott, D. D. *Science* **2008**, *321*, 388.

(22) Constantino, C. J. L.; Lemma, T.; Antunes, P. A.; Aroca, R. *Anal. Chem.* **2001**, *73*, 3674.

(23) Gu, W.; Choi, H.; Kim, K. *J. Phys. Chem. A* **2007**, *111*, 8121.

(24) Jensen, L.; Schatz, G. C. *J. Phys. Chem. A* **2006**, *110*, 5973.

(25) Gu, G. H.; Kim, J. R.; Kim, L.; Suh, J. S. *J. Phys. Chem. C* **2007**, *111*, 7906.

(26) Sauer, G.; Brehm, G.; Schneider, S.; Graener, H.; Seifert, G.; Nielsch, K.; Choi, J.; Gosele, U.; Miclea, P.; Wehrspohn, R. B. *J. Appl. Phys.* **2005**, *97*, 024308.

(27) Wang, H. H.; Liu, C. Y.; Wu, S. B.; Peng, C. Y.; Chan, T. H.; Hsu, C. F.; Wang, J. K.; Wang, Y. L. *Adv. Mater.* **2006**, *18*, 491.

(28) Lee, S. J.; Morrill, A. R.; Moskovits, M. *J. Am. Chem. Soc.* **2006**, *128*, 2200.

(29) Gu, G. H.; Suh, J. S. *Langmuir* **2008**, *24*, 8934.

(30) Zong, R. L.; Zhou, J.; Li, Q.; Du, B.; Li, B.; Fu, M.; Qi, Z.; Li, L.; Buddhudu, S. *J. Phys. Chem. B* **2004**, *108*, 16713.

(31) Osawa, M.; Matsuda, N.; Yoshii, K.; Uchida, I. *J. Phys. Chem.* **1994**, *98*, 12702.

(32) Ruths, M. *Langmuir* **2003**, *19*, 6788.

JP902714T